



This open access document is published as a preprint in the Beilstein Archives with doi: 10.3762/bxiv.2019.102.v1 and is considered to be an early communication for feedback before peer review. Before citing this document, please check if a final, peer-reviewed version has been published in the Beilstein Journal of Organic Chemistry.

This document is not formatted, has not undergone copyediting or typesetting, and may contain errors, unsubstantiated scientific claims or preliminary data.

Preprint Title Synthesis, structural characterization and biological activity of new pyrazolo[4,3-e][1,2,4]triazine acyclonucleosides

Authors Mariusz Mojzych, Zbigniew Karczmarzyk, Joanna Matysiak and Andrzej Fruziński

Publication Date 09 Sep 2019

Article Type Full Research Paper

Supporting Information File 1 SUPPLEMENTARY_MATERIALS-06-09-2019-final.doc; 5.6 MB

ORCID® IDs Mariusz Mojzych - <https://orcid.org/0000-0002-9884-6068>; Zbigniew Karczmarzyk - <https://orcid.org/0000-0003-1740-4354>

Synthesis, structural characterization and biological activity of new pyrazolo[4,3-*e*][1,2,4]triazine acyclonucleosides

Mariusz Mojzych^{a*}, Zbigniew Karczmarzyk^a, Joanna Matysiak^b, Andrzej Fruziński^c

^a *Siedlce University of Natural Sciences and Humanities, Department of Chemistry, ul. 3 Maja 54, 08-110 Siedlce, Poland*

^b *University of Life Sciences, Department of Chemistry, Akademicka 15, 20-950, Lublin, Poland*

^c *Technical University, Department of General and Ecological Chemistry, ul. Żeromskiego 115, 90-924 Łódź, Poland*

Abstract: A series of new pyrazolo[4,3-*e*][1,2,4]triazine acyclonucleosides **2-5** and **8** were prepared and evaluated for their anticancer activity against human cancer cell lines (MCF-7, K-562) and CDK2/E as well as Abl protein kinases inhibitors. Lipophilicity of the compounds was determined using C-18 and IAM chromatography. In order to confirm molecular structures and synthesis pathway of new acyclonucleosides X-ray analysis was performed for model compound **3**. Theoretical calculations at DFT/B3LYP/6-311++G(d,p) level were used for characterization electronic structures of **1-8**. The potential antiviral activity of acyclonucleoside **2-8** was tested *in silico* using molecular docking method.

Keywords: Acyclonucleosides, Pyrazolo[4,3-*e*][1,2,4]triazine, Anticancer activity, X-ray analysis, Theoretical calculation, Molecular docking

* Corresponding author: Tel: +48-025-643 1113; E-mail: mjojzych@yahoo.com.

1. Introduction

The discovery and use of aciclovir (**1**)¹ in medicine as useful and selective antiviral therapeutic agent and the development of viral diseases made the synthesis of new acyclic nucleosides still relevant and very interesting subject of study. The modification of the guanine moiety and the acyclic side chain in aciclovir generated several new compounds of significant antiviral activity e.g. ganciclovir (**2**)², penciclovir (**3**)³, and famciclovir (**4**)⁴ (Fig. 1). To increase oral bioavailability of acyclonucleosides some of them were converted to prodrug forms using valine for esterification. Known in the medical drugs of this group are: valganciclovir (**5**)⁵ and valaciclovir (**6**)⁶ (Fig 1).

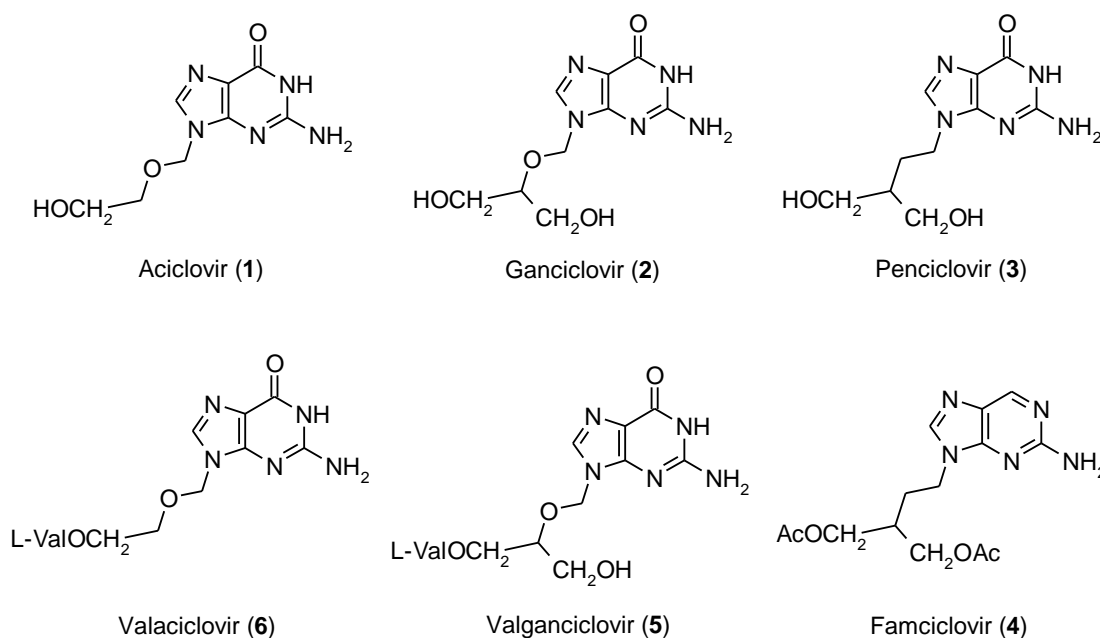


Figure 1. Known acyclonucleosides.

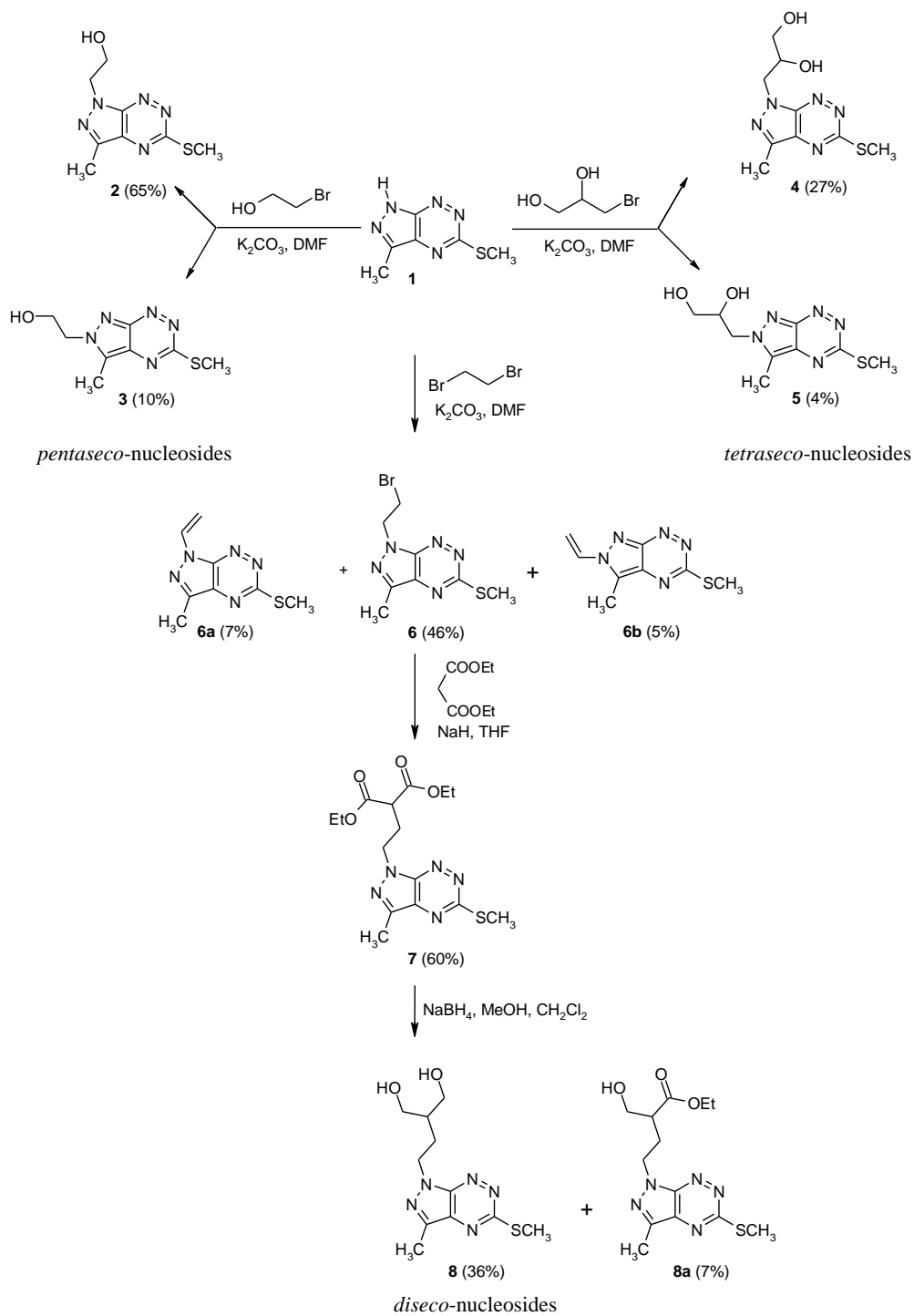
Despite the many research papers devoted to the new acyclonucleosides, very little information is given in literature about acyclonucleosides with pyrazolo[4,3-*e*][1,2,4]triazine ring system^{7,8}, which can be considered as bioisosteric to purine with a wide range of biological activities.

Naturally occurring pyrazolo[4,3-*e*][1,2,4]triazine derivatives are produced by the microorganisms and showed anticancer and antibacterial activity.⁹⁻¹¹ Based on our earlier results related to synthesis and functionalization of pyrazolo[4,3-*e*][1,2,4]triazine core^{12,13} and continuing our work on the preparation of acyclonucleosides^{7,8}, here we will discuss

synthesis, structure and biological activity of new acyclonucleosides containing pyrazolo[4,3-*e*][1,2,4]triazine moiety. A key feature of this strategy is outlined in Scheme 1.

2. Results and discussion

2.1. Chemistry



Scheme 1. Synthetic pathway to pyrazolo[4,3-*e*][1,2,4]triazine acyclonucleosides.

The starting 3-methyl-5-methylsulfanyl-1*H*-pyrazolo[4,3-*e*][1,2,4]triazine (**1**) was synthesized from 5-acetyl-3-methylsulfanyl-1,2,4-triazine in one-pot reaction by condensation with hydrazine hydrochloride, followed by acid-promoted ring closure of the resulting intermediate.¹⁴ The target acyclonucleosides **2-5** were prepared using previously described methods for the synthesis of *N*-alkylated 1*H*- and 2*H*-pyrazolo[4,3-*e*][1,2,4]triazine derivatives.¹⁴ The synthesis was achieved by the reaction of **1** with appropriate alkylating agents in the presence of K₂CO₃ in DMF stirring the reaction mixture at room temperature overnight. The isomeric products were isolated by column chromatography. Compound **8** was synthesized in three steps from 3-methyl-5-methylsulfanyl-1*H*-pyrazolo[4,3-*e*][1,2,4]triazine (**1**). First, derivative **1** was reacted with dibromoethane in the presence of potassium carbonate in DMF to give as a main product **6** with 46% yield and small amount byproducts **6a** and **6b**. In the next step pyrazolotriazine **6** was reacted with diethylmalonate and undergo nucleophilic substitution reaction to yield intermediate **7** in good yield. Treatment of the resulting 1*H*-pyrazolo[4,3-*e*][1,2,4]triazine **7** with sodium borohydrate in mixture of MeOH and CH₂Cl₂ in the ratio 1:1 gave final analogue of penciclovir **8** and derivative **8a** as minor product in 7% yield. The newly synthesized compounds were characterized by ¹H NMR spectroscopy, HR-MS mass spectrometry, and elemental analysis. The spectral data confirmed that all of the new compounds had the expected structures and were of high purity.

2.2. Cytotoxic activity

With respect to our recent studies on anticancer activity of sulfonamide derivatives of pyrazolo[4,3-*e*][1,2,4]triazines observed in vitro in cell lines expressing fusion oncoprotein BCR-Abl,¹⁵ we have evaluated the cytotoxicity of the new acyclonucleosides against two human cancer cell lines; breast adenocarcinoma-derived MCF7 and chronic myelogenous leukemia K562. The results presented in Table 1 demonstrate that none of the compounds possessed cytotoxicity within the tested concentration range. In addition, we have also assayed the new compounds for inhibition of protein kinases CDK2/cyclin E and Abl as described previously.¹⁵ However, in contrast to previously described 5-anilino-pyrazolo[4,3-*e*][1,2,4]triazines that inhibited Abl kinase in micromolar concentrations, none of the new tested compounds proved the ability to inhibit any kinase (Table 1). It could be due to the lack of a NH group between the heterocyclic core and the phenyl ring that is responsible for binding to the kinase.

Table 1. Protein kinase inhibitory activity and the cytotoxic activity of tested pyrazolo[4,3-*e*][1,2,4]triazines and standard after 72 h incubation.

Compd	MTT assay, IC ₅₀ (μM)		IC ₅₀ (μM)	
	K-562	MCF7	CDK2/cyclin E	Abl
1	>100	>100	>100	>100
2	>100	>100	>100	>100
3	>100	>100	>100	>100
4	>100	>100	>100	>100
6	>100	>100	>100	>100
7	>100	>100	>50	>50
8	>100	>100	>100	>100
roskovitin	42	11	0.1	>100
imatinib	0.5	>10	>100	0.2

2.3. Lipophilicity

The UV-Vis spectra in water (phosphate buffer) - methanol solutions of different pH of compounds (**1**) and (**2**) are presented in Fig. 2. They show that pH influences on the electronic structure in the case of compound **1**, and there are no significant changes for other compounds at pH 4 and 7.4 (Fig. 2, compound **2**). As pH = 7.4 is recommended for IAM chromatography measurements, other chromatographic studies were performed at this pH (physiological pH). For comparison C-18 chromatography was made at pH = 4.

The regular retention changes of compounds in the function of organic modifier in the mobile phase was found for RP-18 as well as IAM chromatography. That dependence is expressed by the Soczewiński-Wachtmeister equation¹⁶ :

$$\log k = \log k_w + S (\% \text{ organic modifier}) \quad (\text{Eq. 1})$$

in which $\log k_w$ - intercept and S – slope of the regression curve. $\log k_w$ expresses the retention factor of a solute with pure water as the mobile phase. Parameters: $\log k_w$ obtained by extrapolation technique and S are commonly used as lipophilicity descriptors¹⁷⁻²⁰. The

obtained data are presented in Tables 2 and 3. The dependence between the $\log k_w$ values obtained on octadecyl stationary phase for different pH mobile phase is expressed by Eq. 2.

$$\log k_{w(7.4)} = 0.883 (\pm 0.276) \log k_{w(4)} + 0.155 (\pm 0.526) \quad (\text{Eq. 2})$$

$$n = 6; R = 0.976; s = 0.170; F = 78.98; p = 0.001; Q^2 = 0.867$$

Compound **1** is outlier. Its behavior explains the influence of pH on electronic structure of molecule as well as on the retention in the chromatographic systems.

Some molecular descriptors of compounds were estimated *in silico* (Table 3). The molar refractivity (MR) and $\log P$ values were calculated according to the fragmentation method introduced by Crippen.²¹ For comparison, Clog P was determined. The data show that compounds under consideration possess a low distribution coefficient expressed by $\log P$ as well as by $\log k_w$ values. It can be assumed that low lipophilicity of compounds is not conducive to biological potency.

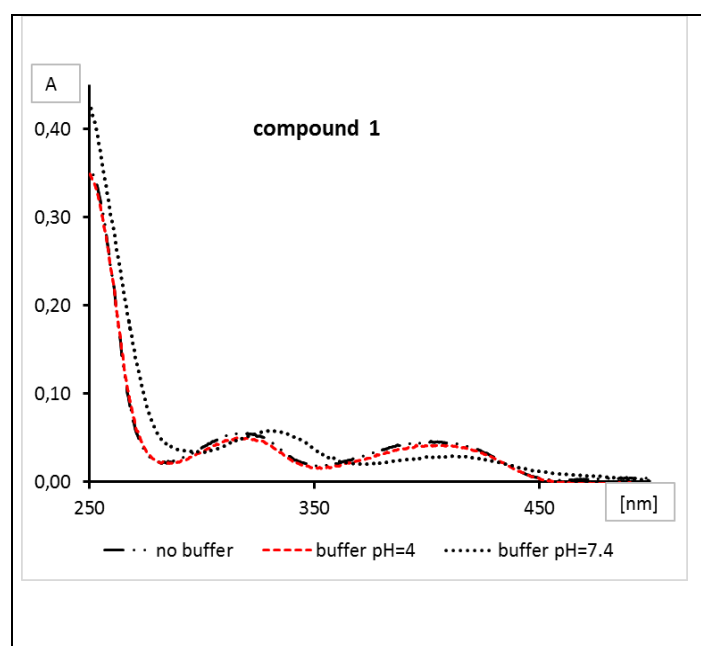
Table 2. Lipophilicity parameters of compounds: $\log k_w$ and $-S$ values (Eq. 1) obtained by RP-18 HPLC chromatography.

Compd	pH = 7.4				pH = 4			
	S	$\log k_w$	R^2	n	S	$\log k_w$	R^2	n
1	-5.268	2.154	0.967	6	-2.7085	1.328	0.979	7
2	-2.995	1.363	0.999	7	-3.1443	1.482	0.978	5
3	-2.895	1.067	0.999	7	-2.8277	1.013	0.979	5
4	-3.005	1.234	0.999	8	-2.8277	1.013	0.979	7
6	-3.494	2.271	0.997	5	-3.7314	2.485	0.976	5
7	-4.231	2.848	0.996	9	-4.150	2.856	0.978	7
8	-3.282	1.579	0.997	7	-3.649	1.828	0.988	5

Table 3. Log $k_{w(IAM)}$ and S parameters of Eq. 1 for compounds obtained by IAM chromatography and their *in silico*:

Compd	IAM chromatography			molecular descriptors ^a				
	S	log $k_{w(IAM)}$	R^2	n	log P	MR (cm ³ /mol)	tPSA (Å ²)	Clog P
1	-3.097	0.667	0.984	8	1.58	50.33	61.47	1.042
2	-2.809	0.435	0.989	9	1.40	61.5	72.91	-0.189
3	-2.580	0.292	0.977	9	1.86	-	72.91	-0.189
4	-2.591	0.275	0.980	9	0.86	67.56	93.12	-0.514
6	-4.132	1.413	0.996	8	2.75	67.6	52.68	1.235
7	-5.286	1.831	0.995	9	2.59	96.27	105.28	1.245
8	-3.181	0.587	0.971	9	1.21	76.84	93.14	-0.830

^a the log P (two different approaches), molar refractivity (MR), tPSA – polar surface area



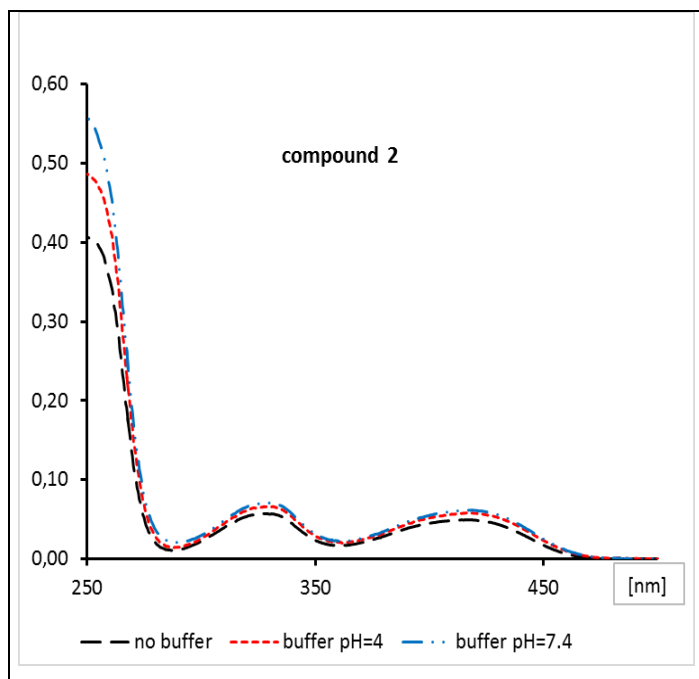


Figure 2. UV–Vis spectra of compounds **1** and **2** in methanol water solution of different pH.

2.4. X-ray analysis

The structure of the synthesized acyclonucleosides was unambiguously established by X-ray crystallography, taken 2-(2-hydroxyethyl)-3,5-dimethyl-2*H*-pyrazolo[4,3-*e*][1,2,4]-triazine (**3**), as a model compound. Crystal structure determination of (**3**) confirmed its assumed molecular structure and synthesis pathway. The structure of compound (**3**) is shown in Fig 3. The bond distances and angles in molecule of (**3**) are in normal ranges and they are comparable to the corresponding values observed in closely related structure of 1,3-dimethyl-5-methylsulfonyl-1*H*-pyrazolo[4,3-*e*][1,2,4]triazine.²² The 2-hydroxyethyl substituent has a *gauche-gauche* conformation with the torsion angles N7-N8-C10-C11 of 82.0(2)° and N8-C10-C11-O1 of 61.3(2)°. The methylthio substituent lies almost in the plane of the triazine ring with the torsion angle N2-C3-S1-C13 of 179.98(15)°.

The packing of the molecules in the crystal structure of (**3**) is governed by O1-H1...N2^{*i*} intermolecular hydrogen bond, linking the molecules into molecular chains parallel to the [101] direction; O1-H1 = 0.86(3), H1...N2 = 2.07(3), O1...N2 = 2.928(2) Å, O1-H1...N2 = 176(3)° and (*i*) = 1/4+*x*, 1/4-*y*, -3/4+*z*. Moreover, the π -electron systems of the pairs of pyrazole and triazine rings belonging to the translation-related molecules overlap each other, with centroid-to-centroid separation of 3.5060(11) Å between the prazole ring at (*x*, *y*, *z*) and triazine ring at (*x*, *y*, -1+*z*) and triazine ring at (*x*, *y*, *z*) and pyrazole ring at (*x*, *y*, 1+*z*). The

$\pi\cdots\pi$ distances are 3.4112(8) and 3.3995(7) Å, respectively and the angle between overlapping planes is 0.84(10)°.

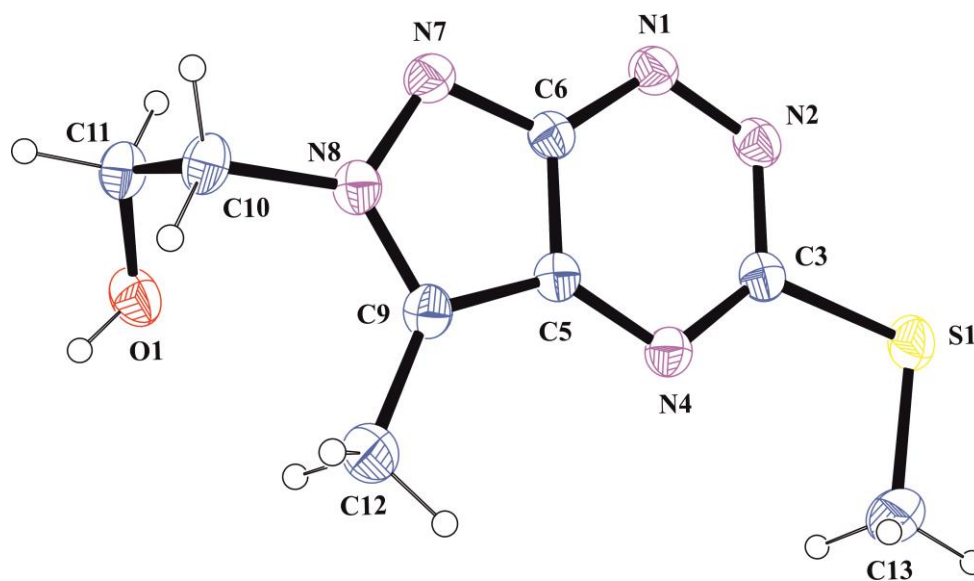


Figure 3. A view of the molecule (**3**), showing the atom-numbering scheme. Displacement ellipsoids are drawn at the 50% probability level.

2.5. Theoretical calculations

The electronic parameters (Table 4) were theoretically calculated at the DFT/B3LYP/311++G(d,p) level for compounds **1–8** in the conformation of the molecules corresponding to the minimum energy. The molecules **1–8** in conformation obtained after energy minimization and geometry optimization with vectors of dipole moment are shown in Fig. 4.

Table 4. Total energy, E_T (kcal/mol.), dipole moment, MD (D), energy of HOMO, E_{HOMO} , and LUMO, E_{LUMO} , orbitals (kcal/mol), $\Delta E = E_{LUMO} - E_{HOMO}$ (kcal/mol) and ionization potential, IP (kcal/mol), for **1–8** calculated at DFT/B3LYP/6-311++G(d,p) level.

Comp.	E_T	MD	E_{HOMO}	E_{LUMO}	ΔE	IP
1	-594977.010	3.100	-149.433	-65.448	83.985	149.433
2	-664394.616	3.791	-146.860	-63.817	83.043	146.860
3	-664388.197	8.420	-142.173	-59.619	82.554	142.173
4	-736287.198	3.993	-143.246	-59.506	83.740	143.246
5	-736278.707	7.582	-142.619	-60.039	82.580	142.619
6	-2232635.401	3.992	-149.941	-67.393	82.548	149.941
7	-1023996.125	3.361	-146.948	-64.155	82.793	146.948
8	-823197.681	6.008	-146.672	-63.779	82.893	146.672

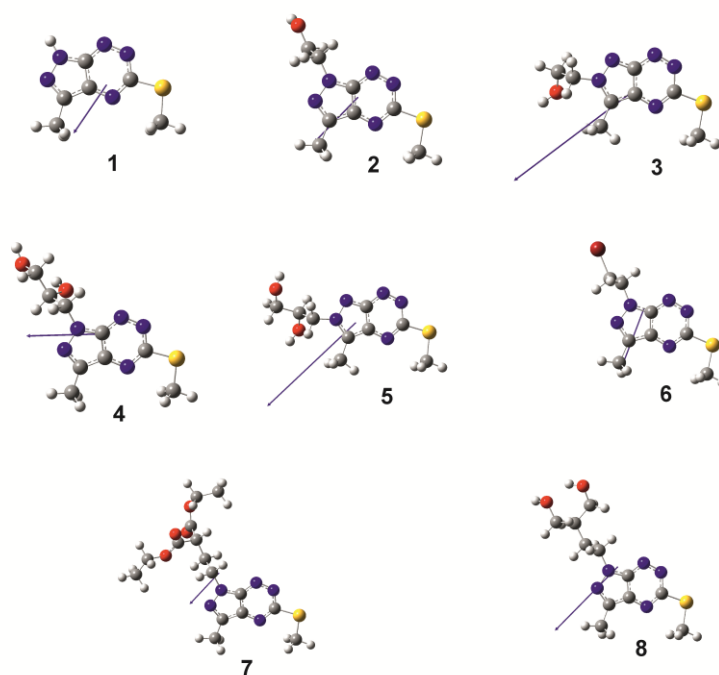


Figure 4. The molecules **1–8** with the vectors of dipole moment in the low-energy conformation obtained from calculations at the DFT/B3LYP/6-311++G(d,p) level.

Theoretical calculations showed that N-1-isomeric forms for compounds **2** and **4** have lower total energy than respective N-2-isomeric forms for **3** and **5**. Moreover, the N-2-substituted pyrazolo[4,3-*e*][1,2,4]-triazine derivatives are more polar than those substituted at

N-1 position. The dipole moments of molecules **1–8** vary from 3.100 D for **1** to 8.420 D for **3**. The vectors of dipole moments have similar spatial orientation for all molecules being roughly parallel to the pyrazolo[4,3-*e*][1,2,4]-triazine system.

In order to characterize the reactivity and stability of investigated compounds the frontier orbitals HOMO and LUMO, as the reactivity descriptors for molecules **1–8** were calculated. The energies of HOMO, LUMO and energy gaps for all investigated compounds are presented in Table 4 and their graphical representation is shown in Fig. 1S (Supplementary materials). The energies of HOMO and LUMO orbitals for all investigated compounds are very close to each other, changing in the range of 7.75 and 5.94 kcal/mol for E_{HOMO} and E_{LUMO} , respectively. Similarly, the energy gaps are within a very narrow range of 1.437 kcal/mol. This may indicate similar reactivity of the tested compounds and their similar behaviour under physiological conditions.

The net charge on the atoms in the 3-methyl–5-methylsulfanyl-1*H*-pyrazolo[4,3-*e*][1,2,4]triazine part of the molecules **1–8** calculated using NBO method is presented in Table 5. The atomic charges are very similar in all analysed molecules, however it can be seen that introduction of the substituent in N-1 or N-2 position of the pyrazolo[4,3-*e*][1,2,4]triazine rings system decreases the absolute value of negative atomic charge on N7 and N8 atoms, respectively, in comparison with the values of the net charge at these atoms observed in **1**. As expected, relatively large negative charges are observed at nitrogen and carbon atom of methylene groups, while large positive charges are present at sulphur and other carbon atoms.

Table 5. Net atomic charges (e) on the atoms in the 3-methyl-5-methylsulfanyl-1*H*-pyrazolo[4,3-*e*][1,2,4]triazine system of molecules **1–8** calculated using NBO method at the DFT/B3LYP/6-311++G(d,p) level.

Atom	1	2	3	4	5	6	7	8
N1	-0.189	-0.193	-0.145	-0.188	-0.147	-0.193	-0.197	-0.194
N2	-0.256	-0.257	-0.250	-0.258	-0.250	-0.254	-0.258	-0.257
C3	+0.215	+0.213	+0.216	+0.214	+0.216	+0.213	+0.214	+0.213
N4	-0.463	-0.462	-0.478	-0.463	-0.478	-0.468	-0.461	-0.462
C5	+0.122	+0.121	+0.081	+0.122	+0.001	+0.123	+0.123	+0.122
C6	+0.288	+0.306	+0.251	+0.315	+0.252	+0.308	+0.306	+0.305
N7	-0.357	-0.234	-0.286	-0.228	-0.289	-0.237	-0.230	-0.230
N8	-0.234	-0.236	-0.167	-0.238	-0.162	-0.237	-0.231	-0.235
C9	+0.148	+0.147	+0.175	+0.150	+0.174	+0.152	+0.148	+0.145
C12	-0.604	-0.602	-0.617	-0.602	-0.616	-0.603	-0.602	-0.602
S1	+0.300	+0.296	+0.302	+0.293	+0.302	+0.301	+0.296	+0.296
C13	-0.701	-0.701	-0.703	-0.701	-0.703	-0.701	-0.701	-0.701

2.6. Molecular docking

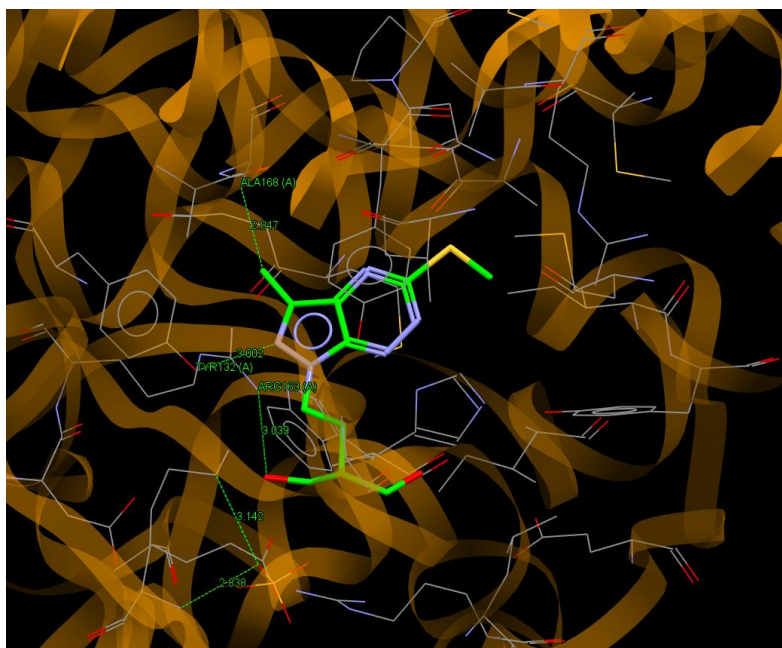
The lack of significant anti-cancer activity of investigated compounds and their structural similarity to the antiviral drug aciclovir prompted us to try to check *in silico* the antiviral activity of acyclonucleosides **1–8** using molecular docking procedure. The compounds **1–8** were tested in virtual screening to the thymidine kinase TK. This enzyme is responsible for the antiviral activity of aciclovir, converting it into a virus-infected cell to an active phosphate derivative that inhibits DNA synthesis and blocking the viral replication process.²³ In crystalline state, TK occurs in the complex with acyclovir, wherein its hydroxyethoxymethyl group has two possible locations in the binding site of TK. The crystal structure of TK with location of acyclovir molecule in active sites is showed in Fig. 3S (Supplementary materials).²³

The molecular docking results obtained for **1–8** and aciclovir molecule (**Ac**) are presented in Table 5. Graphical presentation of interactions between **1–8**, **Ac** and amino acids in the active site of TK enzyme is shown in Fig. 1S (Supplementary materials).

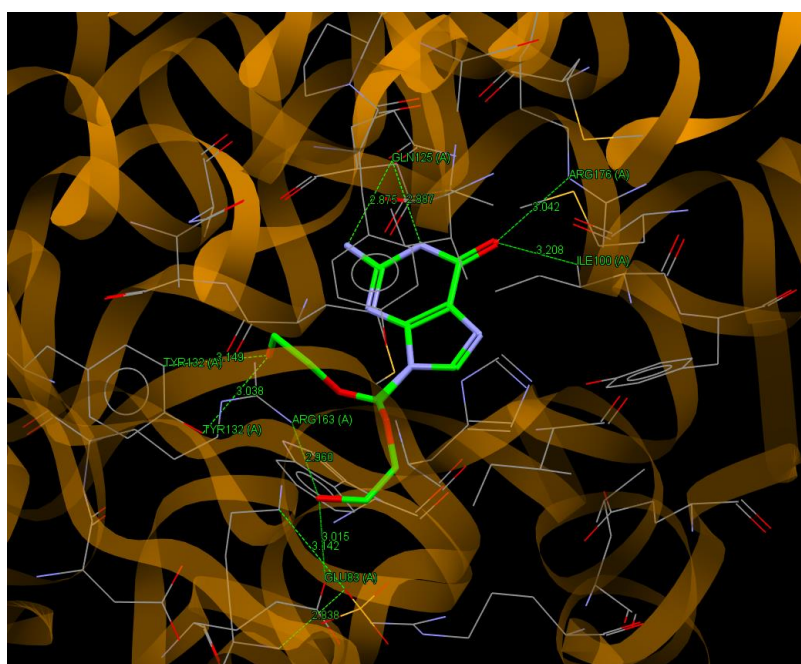
Table 5. The results of the molecular docking of ligands **1–8** and aciclovir molecule (**Ac**) to the TK.

Comp.	ChemPLP score	Interactions
1	43.24	-
2	54.01	-
3	54.93	C13...O (GLN125A); N1...O (TYR132A); O...O (GLU83A); O...N (ARG163A)
4	64.17	O...O (GLN125A); O...N (GLN125A); O'...N (ARG176A)
5	58.68	S1...C(MET128A); S1...C (ALA168A); S1...C (ALA169A); C13...O (GLN 125A); N1...O (TYR132A); O...O (GLU225A)
6	55.22	-
7		S1...C (ILE100A); O...C (MET128A); O'...N (ARG163A); C...N (LYS62A); C'...O (ASP162A)
8	64.74	C12...C (ALA168A); N8...O (TYR132A); O...N (ARG163A)
Ac	77.94	N(amino)...O (GLN125A); N1...O (GLN125A); O6...N (ARG176A); O(hydroxy)...C (TYR132A); O(hydroxy)...O(TYR132A); O(hydroxy)...O (GLU83A); O(hydroxy)...N (ARG163A)

It can be noted that all analysed ligands bind to the active site of TK with the values of scoring function ChemPLP included in the narrow range from 43.24 for **1** (without acyclic side chain) and 53.74 for **7** to 64.74 for **8** and 77.94 for **Ac**, showing that all acyclonucleosides have similar affinity to TK enzyme. The best affinity to the binding site of TK exhibits ligand **8** which binds with ALA168A, TYR132A and ARG163A via C12...C, N8...O and O...N hydrogen bonds, respectively, involving atoms from both bicyclic part and acyclic chain of molecule (Fig. 5a). In similar way as **8**, the molecule of **Ac** is linked to the active pocket of enzyme, but it should be noted that there are two possible position of the acyclic chain of **Ac** molecule in the crystal structure of TK Fig. 5b).



(a)



(b)

Figure 5. A view of the interaction of (a) **8** and (b) **Ac** with amino acids of binding site in TK.

The molecular docking study showed that new obtained acyclonucleosides **2–8** can be considered as the compounds with potential antiviral activity by joining to the thymidine

kinase and subsequently blocking the viral replication process. Experimental studies verifying this thesis are in progress.

3. Conclusions

In summary, new pyrazolo[4,3-*e*][1,2,4]triazine acyclonucleosides were designed and synthesized as a representative of new structural class of novel therapeutic agents. Using alkylation reaction we have produced a new series of prazolotriazine acyclonucleosides with different acyclic chains mimicking the sugar portion of naturally occurring nucleosides. The molecular structure of the model compound **3** was confirmed using X-ray analysis. Theoretical calculations performed at DFT/6-311++G(d,p) level showed that all investigated acyclonucleosides are characterized by similar reactivity and stability and they should therefore behave similarly under physiological conditions. The investigated compounds tested in vitro against human cancer cell lines (MCF-7, K-562) and CDK2/E as well as Abl protein kinases inhibitors showed no significant anticancer activity. However the structural similarity of acyclonucleosides **2–8** to antiviral drug aciclovir encouraged us to check in silico their antiviral activity using molecular docking procedure. The molecular docking of 1 – 8 to thymidine kinase TK revealed that all acyclonucleosides have similar affinity as aciclovir to active site of TK. Further development of this series of compounds and their biological activities will be reported in the future in the separate paper.

4. Experimental

4.1. Chemistry

All the reagents were analytical reagent or chemical pure. Melting points were determined on a Mel-Temp apparatus and are uncorrected. ¹H- and ¹³C-NMR spectra were recorded on a Varian spectrometer (400 MHz for ¹H and 100 MHz for ¹³C). The chemical shift values are expressed in ppm (part per million) with TMS as internal reference. The relative integrals of peak areas agreed with those expected for the assigned structures. Molecular weight of final compounds were assessed by electrospray ionization mass spectrometry (ESI/MS) on a Agilent Technologies 6538 UHD Accurate Mass Q-TOF LC/MS. Elemental compositions are within ±0.4% of the calculated values.

General procedure for the preparation of derivatives 2-5

A mixture of potassium carbonate (607 mg, 4.4 mmol) and derivative **1** (400 mg, 2.2 mmol) in anhydrous DMF (30 mL) was stirred for 10-15 min at room temperature. Then, a solution

of appropriate alkylation agent: 2-bromoethanol or 3-bromo-1,2-propanediol (4.4 mmol) was added and stirred 3 days at room temperature. The reaction solution was poured over crushed ice (40 g) and the aqueous mixture extracted with diethyl ether (5 x 40 ml). The combined extracts were dried over anhydrous CaCl₂ and evaporated under vacuum to give the required crude products. The crude products were submitted to column chromatography on silica gel using dichloromethane as eluent to give N1 alkylated derivative **2** or **4** as the first product. Further elution with CH₂Cl₂/EtOH (50:1) gives pure N2-alkylated derivative **3** or **5**.

1-(2-hydroxyethyl)-3-methyl-5-methylsulfanyl-1H-pyrazolo[4,3-*e*][1,2,4]triazine (2)

Yellow solid; Yield 65%, m.p. 140 - 143°C. ¹H-NMR (DMSO) δ: 2.48 (s, 3H), 2.59 (s, 3H), 3.88 (q, 2H, J = 11.6 Hz), 4.60 (t, 2H, J = 10.8 Hz), 4.82 (t, 1H, J = 11.6 Hz, OH exchanged with D₂O); ¹H-NMR (CDCl₃) δ: 2.63 (s, 3H), 2.72 (s, 3H), 4.18 (t, 2H, J = 8.0 Hz), 4.74 (t, 2H, J = 8.0 Hz). ¹³C-NMR (CDCl₃) δ: 10.63, 13.59, 50.67, 59.27, 134.21, 139.41, 147.44, 165.71. IR (KBr) cm⁻¹: 873, 1070, 1395, 1433, 2924, 3403. Anal. Calcd. for C₈H₁₁N₅OS: C, 42.65; H, 4.92; N, 31.09. Found: C, 42.52; H, 5.03; N, 31.00.

2-(2-hydroxyethyl)-3-methyl-5-methylsulfanyl-2H-pyrazolo[4,3-*e*][1,2,4]triazine (3)

Yellow solid; Yield 10%; m.p. 176 - 178°C; ¹H-NMR (DMSO) δ: 2.63 (s, 3H), 2.67 (s, 3H), 3.93 (q, 2H, J = 10.8 Hz), 4.60 (t, 2H, J = 10.8 Hz), 5.03 (t, 1H, J = 11.6 Hz, OH exchanged with D₂O); ¹³C-NMR (CDCl₃) δ: 8.789, 13.413, 54.491, 60.262, 133.162, 154.208, 164.967, 182.529. Anal. Calcd. for C₈H₁₁N₅OS: C, 42.65; H, 4.92; N, 31.09. Found: C, 42.48; H, 5.10; N, 29.89.

1-(2,3-dihydroxypropyl)-3-methyl-5-methylsulfanyl-1H-pyrazolo[4,3-*e*][1,2,4]triazine (4)

Yellow solid; Yield 27%; m.p. 150°C; ¹H-NMR (DMSO) δ: 2.55 (s, 3H), 2.57 (s, 3H), 3.46 (t, 2H, J = 11.2 Hz), 4.04 (bs, 1H), 4.49–4.61 (m, 2 H), 4.81 (bs, 1H), 4.83 (bs, 1H). ¹H-NMR (DMSO + D₂O) δ: 2.49 (s, 3H), 2.59 (s, 3H), 3.45 (d, 2H, J = 5.6 Hz), 4.02 (m, 1H), 4.50 (d, 2H, J = 7.6 Hz). ¹³C-NMR (CDCl₃) δ: 10.64, 13.59, 51.56, 63.61, 70.11, 134.15, 139.30, 147.52, 165.64. Anal. Calcd. for C₉H₁₃N₅O₂S: C, 42.34; H, 5.13; N, 27.43. Found: C, 42.22; H, 5.25; N, 27.32.

2-(2,3-dihydroxypropyl)-3-methyl-5-methylsulfanyl-2H-pyrazolo[4,3-*e*][1,2,4]triazine (5)
Yellow solid; Yield 4%; m.p. 175°C; ¹H-NMR (acetone+D₂O) δ: 2.56 (s, 3H), 2.59 (s, 3H), 3.52 (d, 2H, J = 12 Hz), 4.09–4.11 (m, 1H), 4.50 (d, 2H, J = 24.4 Hz); ¹³C-NMR (CDCl₃) δ: 8.16, 13.42, 54.88, 63.76, 71.70, 128.55, 133.37, 154.79, 165.63. Anal. Calcd. for C₉H₁₃N₅O₂S: C, 42.34; H, 5.13; N, 27.43. Found: C, 42.18; H, 5.30; N, 27.22.

Reaction of 1 with dibromoethane

To a solution of **1** (1,5 g, 8,28 mmola) in DMF (60 mL), potassium carbonate (2,39 g, 0,017 mmola) was added and the resulting mixture was stirred for 10-15 min. at room temperature. Then, dibromoethane (3 ml, 0,044 mmol) was added and the reaction mixture was stirred for 3 days at room temperature. After that time, reaction mixture was poured into ice-water mixture and extracted with diethyl ether (5 x 40 ml). The combined organic extracts were dried over anhydrous CaCl₂. After complete evaporation of the solvent, the residue was subjected to column chromatography eluting with methylene chloride to give **6a** as the first product. Further elution with CH₂Cl₂/hexane (5:1) gives pure **6** and **6b**.

1-(2-bromoethyl)-3-methyl-5-methylsulfanyl-1H-pyrazolo[4,3-*e*][1,2,4]triazine (6)

Yellow solid; Yield 46%; m.p. 94°C; ¹H-NMR (CDCl₃) δ: 2.63 (s, 3H), 2.72 (s, 3H), 3.88 (t, 2H, J = 13.2 Hz), 4.97 (t, 2H, J = 13.2 Hz); ¹³C-NMR (CDCl₃) δ: 10.97, 14.26, 28.71, 49.31, 135.12, 141.49, 147.32, 167.66; IR (KBr) cm⁻¹: 553, 1428, 1547, 2923, 2968, 3404. Anal. Calcd. for C₈H₁₀BrN₅S: C, 33.34; H, 3.50; N, 24.30. Found: C, 33.21; H, 3.49; N, 24.11.

3-methyl-5-methylsulfanyl-1-vinyl-1H-pyrazolo[4,3-*e*][1,2,4]triazine (6a)

Yellow solid; Yield 7%; m.p. 88°C; ¹H-NMR (CDCl₃) δ: 2.64 (s, 3H), 2.73 (s, 3H), 5.08 (dd, 1H, J₁ = 9.2 Hz, J₂ = 1,2 Hz), 6.09 (d, 1H, J = 15,6 Hz), 7.56 (d, 1H, J = 15.6 Hz); ¹³C-NMR (CDCl₃) δ: 10.95, 14.27, 101.04, 128.85, 136.42, 142.62, 146.22, 168.37; IR (KBr) cm⁻¹: 627, 882, 1457, 1552, 1648, 2927; Anal. Calcd. for C₈H₉N₅S: C, 46.36; H, 4.38; N, 33.79. Found: C, 46.23; H, 4.47; N, 33.63.

3-methyl-5-methylsulfanyl-2-vinyl-2H-pyrazolo[4,3-*e*][1,2,4]triazine (6b)

Yellow solid; Yield 5%; m.p. 197°C; ¹H-NMR (CDCl₃) δ: 2.67 (s, 3H), 2.72 (s, 3H), 5.50 (d, 1H, J = 8.8 Hz), 6.50 (d, 1H, J = 15.2 Hz), 7.37 (dd, 1H, J₁ = 15.2 Hz, J₂ = 1.2 Hz); ¹³C-NMR (CDCl₃) δ: 8.83, 14.04, 111.69, 128.81, 129.65, 131.18, 154.48, 166.81. IR (KBr) cm⁻¹: 852, 1429, 1511, 1631, 2923; Anal. Calcd. for C₈H₉N₅S: C, 46.36; H, 4.38; N, 33.79. Found: C, 46.45; H, 4.51; N, 33.60.

Synthesis of 1-(ethyl 2-carboethoxybutanoate-4-yl)-3-methyl-5-methyl-sulfany-1H-pyrazolo[4,3-*e*][1,2,4]triazine (7)

Intermediate compound **6** (288 mg, 1 mmol) was dissolved in THF (40 mL). To the solution, diethyl malonate (0.8 mL, 0.851 g, 5.32 mmol) and NaH (414 mg, 50% dispersion in mineral oil) were added, followed by stirring for 2 days at room temperature. After completion of the reaction, the solvent was evaporated *in vacuo* and the crude product was submitted to column chromatography on silica gel using a mixture of dichloromethane/hexane (50:1) as eluent to give derivative **7**.

Yellow oil; Yield 60%; ¹H-NMR (CDCl₃) δ: 1.18–1.20 (m, 6H), 2.53 (m, 4H), 2.65 (s, 3H), 2.71 (s, 3H), 3.28 (t, 1H, J = 14.8 Hz), 4.11 (q, 2H, J = 4 Hz), 4.63 (t, 2H, J = 13.2 Hz); ¹³C-NMR (CDCl₃) δ: 11.05, 14.11, 14.37, 28.55, 45.89, 49.39, 61.85, 134.96, 140.97, 147.24, 167.44, 168.61; IR (KBr) cm⁻¹: 657, 1494, 1546, 1732, 2983;

HRMS (ESI, *m/z*) calc. for C₁₅H₂₁N₅O₄S [M⁺] 367.13142. Found 367.13290. Anal. Calcd. for C₁₅H₂₁N₅O₄S: C, 49.03; H, 5.76; N, 19.06. Found: C, 48.87; H, 5.80; N, 18.87.

Reduction of 7

Compound **7** (580 mg, 1.5 mmol) was dissolved in CH₂Cl₂ (8 mL), and MeOH (0.6 mL) and NaBH₄ (330 mg, 9 mmol) were added. The reaction mixture was stirred at room temperature for 24 hs, then diluted with water (8 mL) and extracted with CH₂Cl₂ (5 x 10 mL). The combined organic extracts were dried over anhydrous CaCl₂. After complete evaporation of the solvent, the residue was subjected to column chromatography (methylene chloride/ethyl alcohol, 100:1) to give **8** as the main product and **8a**.

1-[(4-hydroxy-3-hydroxymethyl)butyl]-3-methyl-5-methylsulfanyl-1H-pyrazolo[4,3-*e*][1,2,4]triazine (8)

Yellow oil; Yield 36%; ¹H-NMR (CDCl₃) δ: 1.73–1.71 (m, 1H), 2.03–2.09 (q, 2H, J = 14.4 Hz), 2.55 (bs, 2H), 2.61 (s, 3H), 2.70 (s, 3H), 3.68–3.84 (m, 4H), 4.69 (t, 2H, J = 14.4 Hz). ¹³C-NMR (CDCl₃): 11.05, 14.35, 28.03, 39.70, 46.48, 64.92, 135.09, 140.74, 146.97, 167.30. Anal. Calcd. for C₁₁H₁₇N₅O₂S: C, 46.63; H, 6.05; N, 24.72. Found: C, 46.70; H, 6.23; N, 24.65.

ester etylowy kwasu-[2-hydroksymetylo-4-(3-metylo-5-metylosufanylo-1*H*-pirazolo[4,3-*e*][1,2,4]trazyn-1-yl]butanowego (8a)

Yellow oil; Yield 7%; ¹H-NMR (CDCl₃) δ: 1.57–1.62 (m, 1H), 1.94 (bs, 1H), 2.08–2.12 (m, 2H), 2.62 (s, 3H), 2.72 (s, 3H), 3.67–3.70 (q, 2H, J = 13 Hz), 3.84–3.85 (t, 2H, J = 13 Hz), 4.64–4.68 (t, 2H, J = 14.4 Hz), 4.69–4.72 (m, 3H). ¹³C-NMR (CDCl₃): 10.93, 14.26, 28.09, 44.59, 48.04, 52.06, 61.07, 62.79, 134.86, 140.70, 147.03, 167.30. Anal. Calcd. for C₁₃H₂₀N₅O₃S: C, 47.84; H, 6.18; N, 21.46. Found: C, 47.80; H, 6.32; N, 21.33.

4.2. Pharmacology

4.2.1. Cytotoxicity assays

The cytotoxicity of the studied compounds in K562 and MCF7 cell lines was determined as described earlier.¹⁵ Briefly, the cells were assayed with compounds using three-fold dilutions in triplicate. Treatment lasted for 72 h, followed by addition of Calcein AM solution and measurement of the fluorescence of live cells at 485 nm/538 nm (excitation/emission).

4.2.2. Kinase inhibition assay

Kinase assays were performed as described earlier.¹⁵ CDK2/cyclin E was assayed with 1 mg/mL histone H1 in the presence of 15 μM ATP, 0.05 μCi [^γ-³³P]ATP and of the test compound in a final volume of 10 μL in a reaction buffer (60 mM HEPES-NaOH, pH 7.5, 3 mM MgCl₂, 3 mM MnCl₂, 3 μM Na-orthovanadate, 1.2 mM DTT, 2.5 μg/50 μL PEG_{20.000}). Abl was assayed with 500 μM of a synthetic peptide (GGEAIYAAPFKK) 10 μM of [^γ-³³P]ATP and the appropriate quantity of the test compound in a final volume of 10 μL. The reactions were stopped and spotted onto P-81 phosphocellulose (Whatman) and kinase inhibition was quantified using a FLA-7000 digital image analyzer (Fujifilm).

4.3. Chromatographic studies

4.3.1. UV-Vis spectroscopy

UV-Vis spectra were recorded in water (phosphate buffer) - methanol (1:1) solution on a UV-160A Shimadzu Spectrophotometer. Quartz cuvettes (1 cm) were used for measurements.

4.3.2. RP-18 chromatography

A Eurosil Bioselect C18 (5 μm , 300 \times 4,6 mm) column was used as the stationary phase. The mobile phase consisted of different volume mixtures of: (i) methanol and 20 mM phosphate buffer as the aqueous phase to give pH 7.4; (ii) methanol and 20 mM acetate buffer as the aqueous phase to give pH 4. The methanol concentration ranged from 0.55 to 0.95 (v/v), depending on the structure of compound, at 0.05 intervals. The flow rate was 0.5 mL/min at room temperature. Measurements were made at 320 nm. The retention time of an unretained solute (t_0) was determined by the injection of a small amount of acetone dissolved in water.

4.3.3. IAM chromatography

A Rexchrom IAM.PC.DD2 (12 μm , 100 \times 4.6 mm, 300 \AA) (Regis Technologies) column was used as the stationary phase. The mobile phase consisted of different volume mixtures of acetonitrile and 20 mM phosphate buffer as the aqueous phase to give pH 7.4 (0.02 M KH_2PO_4 , Na_2HPO_4 and 0.15 M KCl). The acetonitrile concentration ranged from 0.1 to 0.5 (v/v), depending on the structure of compound, at 0.05 intervals. The flow rate was 1 mL min^{-1} at room temperature. Measurements were made at 320 nm. The retention time of an unretained solute (t_0) was determined by the injection of a small amount of citric acid dissolved in water.

HPLC measurements were carried out using a liquid chromatograph Knauer (Knauer, Berlin, Germany) with a dual pump and a UV–visible detector.

The Clog P, log P and molar refractivity MR were calculated using the ChemDraw Ultra 10.0 according to the fragmentation method introduced by Crippen.^{21,24} The polar surface area (tPSA) was estimated by the atom-based method using the MarvinViw 5.9.4 software.^{25,26}

4.4. X-ray structure determinations of **3**

X-ray data of **3** were collected on the Bruker SMART APEX II CCD diffractometer; crystal sizes 0.59 \times 0.04 \times 0.03 mm, $\text{CuK}\alpha$ ($\lambda = 1.54178 \text{ \AA}$) radiation, ω scans, $T = 293 \text{ K}$, absorption correction: multi-scan SADABS²⁷, $T_{\text{min}}/T_{\text{max}} = 0.8131/1.0000$. The structure was solved by direct methods using SHELXS97²⁸ and refined by full-matrix least-squares with SHELXL97.²⁸ The O-bound H atom was located by difference Fourier synthesis and refined freely. The remaining H atoms were positioned geometrically and treated as riding on their

parent C atoms with C-H distances of 0.97 Å (CH₂) and 0.96 Å (CH₃). All H atoms were refined with isotropic displacement parameters taken as 1.5 times those of the respective parent atoms. Compound (**3**) crystallizes in non-centrosymmetric space group *Fdd2* and the assumed absolute structure of its crystal was confirmed by the Flack parameter of 0.027(17) for 615 Friedel pairs.²⁹ All calculations were performed using WINGX version 1.64.05 package.³⁰ CCDC-1948479 contains the supplementary crystallographic data for this paper. These data can be obtained free of charge at www.ccdc.cam.ac.uk/conts/retrieving.html [or from the Cambridge Crystallographic Data Centre (CCDC), 12 Union Road, Cambridge CB2 1EZ, UK; fax: +44(0) 1223 336 033; email: deposit@ccdc.cam.ac.uk].

Crystal data of (3): C₈H₁₁N₅OS, *M* = 225.28, orthorhombic, space group *Fdd2*, *a* = 30.0070(9), *b* = 31.8941(1), *c* = 4.36030(10) Å, *V* = 4173.0(2) Å³, *Z* = 16, *d*_{calc} = 1.435 Mg m⁻³, *F*(000) = 1888, *μ*(Cu Kα) = 2.634 mm⁻¹, *T* = 293K, 11154 measured reflections (*θ* range 4.05–69.30°), 1704 unique reflections, final *R* = 0.025, *wR* = 0.067, *S* = 1.047 for 1640 reflections with *I* > 2σ(*I*).

4.5. Theoretical calculations

The energy and electronic parameters (frontier orbitals, dipole moments and NBO net charge distribution on the atoms) for all structures **1–8** were calculated with GAUSSIAN 03³¹ at the DFT/B3LYP level with 6-311++G(d,p) basis set. The initial geometries were built from the crystallographic data of **3** and the structures were fully optimized with energy minimisation. Calculations were carried out at the Academic Computer Centre in Siedlce. The visualization of theoretical calculation results was performed using GaussView.³²

4.6. Molecular docking

The crystal structure of thymidine kinase TK in complex with aciclovir was downloaded from Protein Data Bank (PDB ID: 2KI5).²³ Docking procedures were carried out for **1–8** using the GOLD Suite v. 5.7.2 software.³³ The enzyme preparation including addition of hydrogens, removal of water molecules, extraction of original ligand from the protein binding site, were done with GOLD default settings. The binding pocket of acyclovir molecule in crystal structure of TK was used as an active site with selection of atoms within 6 Å in molecular docking of investigated ligands. The acyclovir as reference ligand was removed from X-ray structure of its protein–ligand complex (2KI5) and docked back into its binding site with the

RMSD values of 2.794 Å. In docking stimulations running with default parameters, each ligand was kept flexible but the amino acid residues of the enzyme were held rigid. ChemPLP scoring function was used to rank of docked ligands. Protein–ligand interactions were analysed using Hermes v. 1.10.2.³³

5. References

1. Schaeffer, H. J.; Beauchamp, L.; De Miranda, P.; Elion, G. B.; Bauer, D. J.; Collins, P. *Nature*. **1978**, *272*, 583-585.
2. Wang, Q.; Sun, Ch.; Xu, B.; Jiasheng, Tu.; Shen, Y. *Drug Delivery* **2018**, *25*, 59–69.
3. Harnden, M. R.; Jarvest, R. L.; Bacon, T. H.; Boyd, M. R. *J. Med. Chem.* **1987**, *30*, 1636-1642.
4. Torii, T.; Shiragami, H.; Yamashita, K.; Suzuki, Y.; Hijiya, T.; Kashiwagi, T.; Izawa, K. *Tetrahedron* **2006**, *62*, 5709-5716.
5. Yu, M. A.; Park, J. M. *Expert Opin Pharmacother.* **2013**, *14*, 807-815.
6. Perry, C. M.; Faulds, D. *Drugs* **1996**, *52*, 754-772.
7. Mojzych, M.; Rykowski, A.; Wierzchowski, J. *Molecules* **2005**, *10*, 1298-1306.
8. Mojzych, M.; Rykowski, A. *Heterocycles* **2007**, *71*, 2449-2456.
9. Linden, H. J.; Schaden, G. *Chem. Ber.* **1972**, *105*, 1949-1955.
10. Hirata, K.; Nakagami, H.; Takashima, J.; Miyamoto, K. *Heterocycles* **1996**, *43*, 1513-1519.
11. Smirnov, V. V.; Kiprianova, E. A.; Garagulya, A. D.; Esipov, S. E.; Dovjenko, S. A. *FEMS Microbiology Lett.* **1997**, *153*, 357-361.
12. Rykowski, A.; Mojzych, M.; Karczmarzyk, Z. *Heterocycles* **2000**, *53*, 2175-2181.
13. Mojzych, M.; Rykowski, A. *Heterocycles* **2004**, *63*, 1829-1838.
14. Mojzych, M.; Rykowski, A. *Polish J. Chem.* **2003**, *77*, 1797-1803.
15. Mojzych, M.; Subertová, V.; Bielawska, A.; Bielawski, K.; Bazgier, V. *Eur. J. Med. Chem.* **2014**, *78*, 217-224.
16. Soczewiński, E.; Wachtmeiser, C. A. *J. Chromatogr. A.* **1962**, *7*, 311-320.
17. Rożyło, J. K.; Matysiak, J.; Niewiadomy, A.; Żabińska, A. *JPC-J Planar Chromat.* **2000**, *13*, 176-181.
18. Valko, K. *J. Chromatogr. A.* **2004**, *1037*, 299-310.
19. Matysiak, J.; Niewiadomy, A.; Senczyna, B.; Żabińska, A.; Rożyło, J. K. *J. AOAC Int.* **2004**, *87*, 579-586.
20. Niewiadomy, A.; Żabińska, A.; Matysiak, J.; Rożyło, J. K. *J. Chromatogr. A.* **1997**, *791*, 237-243.
21. Ghose, A. K.; Crippen, G. M. *J. Chem. Inf. Comput. Sci.*, **1987**, *27*, 21–35.
22. Mojzych, M.; Karczmarzyk, Z.; Wysocki, W. *Acta Cryst.* **2010**, *E66*, o3226.

23. Bennett, M. S.; Wien, F.; Champness, J. N.; Batuwangala, T.; Rutherford, T.; Summers, W. C.; Sun, H.; Wright, G.; Sanderson, M. R.; *FEBS Lett.* **1999**, *443*, 121-125.
24. ChemDraw Ultra 10.0, Cambridge Soft Corporation, Cambridge USA **2006**.
25. Ertl, P.; Rohde, B.; Selzer, P. *J. Med. Chem.* **2000**, *43*, 3714-3717.
26. MarvinViw 5.9.4, ChemAxon Ltd.
27. Bruker (2005). SADABS (Version 2004/1). Bruker AXS Inc., Madison, Wisconsin, USA.
28. Sheldrick, G. M. *Acta Cryst A.* **2008**, *64*, 112-122.
29. Flack, H. D. *Acta Cryst. A.* **1983**, *39*, 876-881.
30. Farrugia, L. J.; *J. Appl. Cryst.* **2012**, *32*, 837-838.
31. Frisch, M. J.; Trucks, G. W.; Schlegel, H. B.; Scuseria, G. E.; Robb, M. A.; Cheeseman J. R.; Montgomery J. A. Jr.; Vreven, T.; Kudin, K. N.; Burant, J. C.; Millam, J. M.; Iyengar, S. S.; Tomasi, J.; Barone, V.; Mennucci, B.; Cossi, M.; Scalmani, G.; Rega, N.; Petersson, G. A.; Nakatsuji, H.; Hada, M.; Ehara, M.; Toyota, K.; Fukuda, R.; Hasegawa, J.; Ishida, M.; Nakajima, T.; Honda, Y.; Kitao, O.; Nakai, H.; Klene, M.; Li, X.; Knox, J. E.; Hratchian, H. P.; Cross, J. B.; Bakken, V.; Adamo, C.; Jaramillo, J.; Gomperts, R.; Stratmann, R. E.; Yazyev, O.; Austin, A. J.; Cammi, R.; Pomelli, C.; Ochterski, J. W.; Ayala, P. Y.; Morokuma, K.; Voth, G. A.; Salvador, P.; Dannenberg, J. J.; Zakrzewski, V. G.; Dapprich, S.; Daniels, A. D.; Strain, M. C.; Farkas, O.; Malick, D. K.; Rabuck, A. D.; Raghavachari, R.; Foresman, J. B.; Ortiz, J. V.; Cui, Q.; Baboul, A. G.; Clifford, S.; Cioslowski, J.; Stefanov, B. B.; Liu, G.; Liashenko, A.; Piskorz, P.; Komaromi, I.; Martin, R. L.; Fox, D. J.; Keith, T.; Al-Laham, M. A.; Peng, C. Y.; Nanayakkara, A.; Challacombe, M.; Gill, P. M. W.; Johnson, B.; Chen, W.; Wong, M. W.; Gonzalez, C.; Pople, J. A. Gaussian 03, Revision E.01, Gaussian, Inc., Wallingford CT, **2004**.
32. Frisch, A. E.; Dennington, R. D. II; Keith, T. A.; Millam, J.; Nielsen, A. B.; Holder, A. J.; Hiscocks, J. Gauss View Reference Gaussian Inc., version 4, Wallingford, USA, 2007.
33. Jones, G.; Willett, G. P.; Glen, R. C.; Leach, A. R.; Taylor, R. *J. Mol. Biol.* **1997**, *267*, 727-748.

Graphical abstract

